JOURNAL OF MATERIALS SCIENCE 31 (1996) 2481–2486

Study of fluorine doping during vapour-phase axial deposition sintering process

M. KYOTO, M. ITO, Y. ISHIGURO, H. KANAMORI, Y. OHOGA, S. ISHIKAWA
R&D Group, Sumitomo Electric Industries, Ltd., 1, Taya-cho, Sakae-ku, Yokohama, 244, Japan

The fluorine doping process of pure silica "soot" with various type of fluorine gases in the vapour-phase axial deposition (VAD) sintering process was investigated in detail. This investigation showed that the doping level is proportional to the 1/4 power of the concentration of the fluorine gas, and the achievable reduction of relative refractive index is -0.75% with this process. The kinetic investigation clarified that the fluorine doping process consists of the doping and dissociation reactions; the former reaction obeys the 1/2 power of the SiF_4 partial pressure and the latter the two power of fluorine content $[SiO_{1.5}F]$, where $SiO_{1.5}F$ represents a silicon tetrahedron consisting of one fluorine and three bridging oxygen atoms in glass. The fluorine content is proportional to the 1/4 power of the SiF_4 partial pressure at an equilibrium where the doping reaction is in competition with the dissociation reaction.

1. Introduction

The most important dopant for preparing a pure silica core fibre is fluorine because this dopant depresses the refractive index of the cladding glass without any additional loss, as opposed to a boron dopant [1].

Fluorine doping has been demonstrated for the fibre fabrication processes by the MCVD (modified chemical vapour deposition) [2, 3], the PCVD (plasma chemical vapour deposition) [4] and the VAD (vapour-phase axial deposition) [5] methods.

As already reported, we have developed fluorine doping during the VAD sintering process and the fluorine doped glass prepared by this process has promising characteristics as a pure silica core single-mode fibre (Si-SMF) [7, 8]. The Si-SMF with this fluorine doped cladding glass showed low attenuation and drastically improved stability under hydrogen and gamma-ray environments, which should be yielded by an "improved" fluorine doped glass [5, 9].

Further applications of fluorine-doped silica glass for various type of fibres and optical components of u.v. submicrometre lithography should require more improved control of manufacturing process of fluorine doping [10, 11]. In order to improve the fluorine doping process, a basic understanding of its doping mechanism is important. The mechanism of fluorine doping process in VAD sintering process is, however, not fully understood, although the authors have proposed a model [12].

In this paper, the detailed investigation of fluorine doping in the VAD sintering process is described. Based on the kinetic investigation, the fluorine doping mechanism is also discussed.

2. Experimental procedure

Porous preforms were synthesized by a single torch as shown schematically in Fig. 1(a). The raw material, $SiCl_4$ was fed into the torch. In the oxyhydrogen flame, fine soot particles were synthesized and the particles were deposited onto the end surface of a starting rod which was rotated while being pulled upwards at the same speed as the soot deposition growth rate. The porous soot was next heated in the gas stream of fluorine source gas and He in an electric furnace at a given temperature as shown schematically in Fig. 1(b), and then consolidated to a transparent glass preform. SF_6, CF_4, C_2F_6 and SiF_4 were used as the fluorine source gases. The glass preform was elongated and jacketed with a pure silica tube, which was used as the reference for refractive index measurement. The fluorine content in porous soot was estimated from the infrared transmission spectrum, in which the peaks at 935 cm^{-1} and 800 cm^{-1}, are corresponding to the Si–F bond and Si–O–Si bonds, respectively [8].

3. Dependence of fluorine doping on process parameters

There are four important parameters in the fluorine doping process; fluorine gas ratio, processing time, processing temperature and fluorine source gas species.

Fig. 2 shows the Arrhenius form of the index depression. The soot preforms were heated for three hours in a partial pressure of SF_6 with 2.026 kPa at a given temperature followed by consolidation in a helium atmosphere at a higher temperature. The index depresses with increasing temperature.

Fig. 3 shows the time dependence of the relative refractive index depression $-\Delta n$. The soot preforms

0022–2461 © *1996 Chapman & Hall*

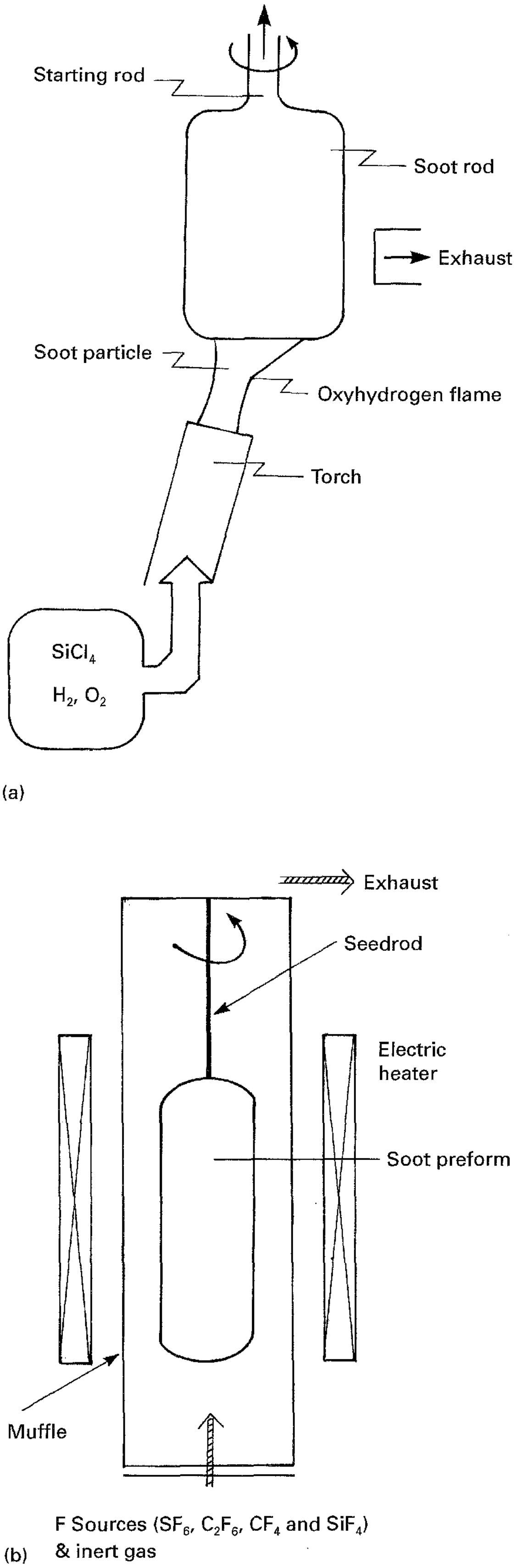

Figure 1 (a) Schematic diagram of the experimental soot deposition. (b) Schematic diagram of fluorine doping in sintering process for basic investigation.

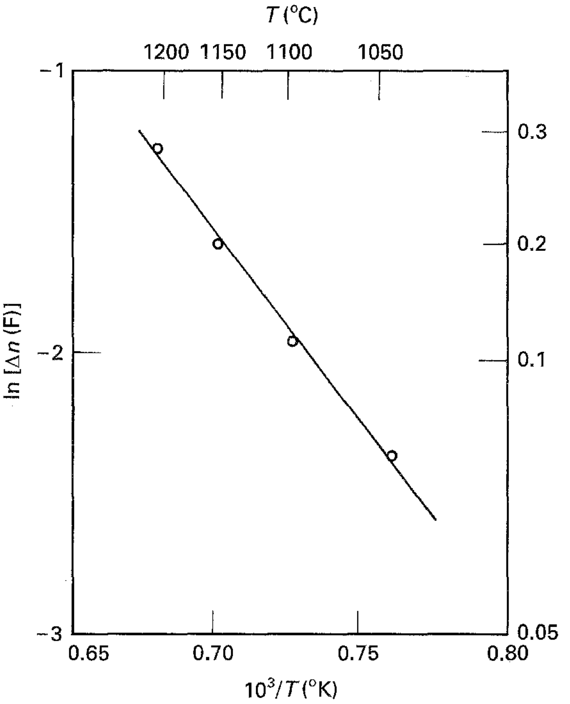

Figure 2 Temperature dependence of Δn(F). $p_{SF_6} = 0.02$, $t = 3$ h.

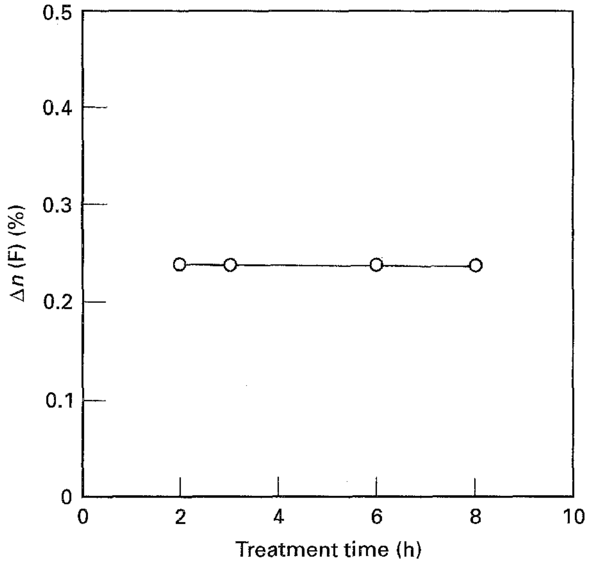

Figure 3 Relationship between treatment time and Δn(F). $p_{SF_6} = 2.02$ kPa, $T = 1150$ °C.

were heated in a partial pressure of SF_6 with 2.026 kPa at 1200 °C followed by consolidation in a helium atmosphere at a higher temperature. There was a tendency for the index depression to saturate after 2 h. This result suggests that the doping reaction attains equilibrium after 2 h of fluorine doping.

Fig. 4 shows the relationship between the index depression and partial pressure of SF_6 in equilibrium state. The soot preforms were heated for three hours at 1200 °C. The index depression $-\Delta n$ is proportional to the 1/4 power of the partial pressure and the maximum index depression is -0.75%. This relation can be expressed by

$$\Delta n = -0.75 \times [p(SF_6)]^{1/4} \qquad (1)$$

where $p(SF_6)$ is partial pressure of SF_6.

Fig. 5 shows the relationship between the index depression and the fluorine source gases. It can be

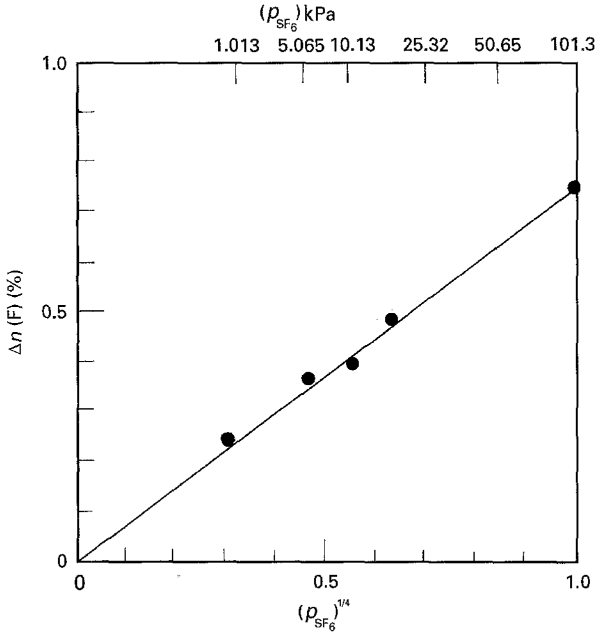

Figure 4 Relationship between p_{SF_6} and Δn(F) where p_{SF_6} is partial pressure of SF_6 ($\Delta n(F) = 0.75\ (p_{SF_6})^{1/4}$, $T = 1200\,°C$, $t = 3$ h).

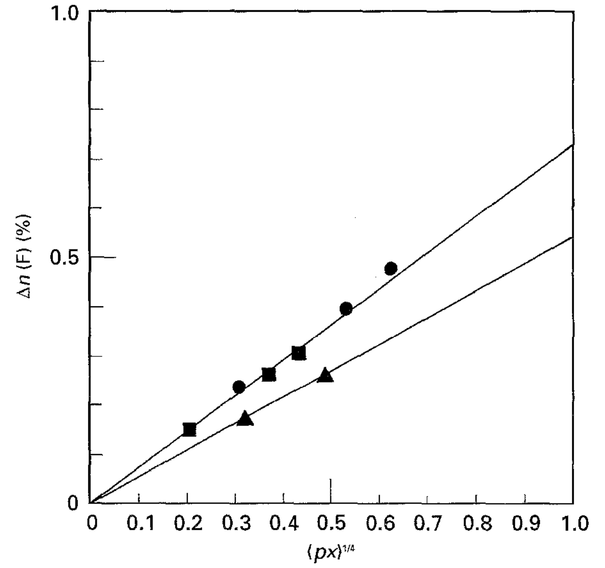

Figure 5 Relationship between px and Δn(F). $T = 1200\,°C$, $t = 3$ h. ● SF_6; ■ C_2F_6; ▲ CF_4.

deduced that the index depression is proportional to the 1/4 power of the fluorine gas partial pressure for any gas species. SF_6 and C_2F_6 appear to be the most effective sources for doping fluorine in glass compared with CF_4.

Based on these results, the relationship between the depressed index and process parameters is summarized in the following equation.

$$\Delta n = -0.75 \times A \times [p(\mathrm{F})]^{1/4} \text{ at } 1200\,°\mathrm{C} \tag{2}$$

where Δn is refractive index relative to silica (%), p(F) is partial pressure of fluorine source gas and A is 1 for SF_6, C_2F_6, 2/3 for CF_4.

From this investigation, it is confirmed that the fluorine doping reaction is proportional to the 1/4 power of the partial pressure of fluorine source gases. Furthermore, it has been identified by Raman and infrared spectroscopic studies that fluorine doping in pure silica glass is caused by oxygen–fluorine substitution in the Si–O network [10]. Then, based on the law of mass action, the following reaction can be derived. For SF_6

$$SF_6 + 6SiO_2 \rightarrow 6SiO_{1.5}F + SO_3 \tag{3}$$

where $SiO_{1.5}F$ represents a silicon tetrahedron consisting of one fluorine and three oxygen atoms. This structure in a fluorine-doped glass has been identified by Raman and infrared spectroscopic studies [9]. From the complex result that the depression value to a partial pressure is different to each fluorine source gases, it can be deduced that Equation 3 consists of the following reactions

$$\begin{aligned} SF_6(g) + 3/2SiO_2(s) &\rightarrow 3/2SiF_4(g) + SO_3(g) \\ CF_4(g) + SiO_2(s) &\rightarrow SiF_4(g) + CO_2(g) \qquad (4) \\ C_2F_6(g) + 3/2SiO_2(s) &\rightarrow 3/2SiF_4(g) + CO(g) \\ &\qquad + CO_2(g) \end{aligned}$$

$$3SiO_2(s) + SiF_4(g) \rightarrow 4SiO_{1.5}F(s) \tag{5}$$

where $SiO_{1.5}F$ represents a silicon tetrahedron consisting of one fluorine and three bridging oxygen atoms. The former reaction is the decomposition reaction of the fluorine sources with SiO_2 resulting in the formation of SiF_4 and the latter is the fluorine doping reaction by SiF_4. Thermochemical calculations show that Equation 4 is towards the right above 1000 °C.

These reactions make it possible to explain clearly the experimental result that the depressed index $-\Delta n$ is proportional to the 1/4 power of the partial pressure of fluorine source gases. However, from the above results, it is difficult to discuss the reaction mechanism in more detail, i.e. whether the fluorine doping reaction is in equilibrium or not.

4. Kinetic study of fluorine doping process

4.1. Kinetic equation

To clarify the mechanism of fluorine doping in the VAD sintering process, the fluorine doping behaviour during sintering was observed in detail.

Fig. 6 shows the time dependence of fluorine content in the soot preforms. The soot preforms were heated in a SiF_4 partial pressure of 4.35 kPa. The fluorine content clearly increases with increasing time. The fluorine content has a tendency toward saturation which is reached more rapidly with increasing temperature. The saturated fluorine content is higher with temperature. This saturation should be caused by the equilibrium between the fluorine doping and dissociating reactions.

The kinetic equation for these reactions can be given as the following Arrhenius form, in which the doping and dissociating rates are postulated to be proportional to nth order of $[SiF_4]$ and mth order of

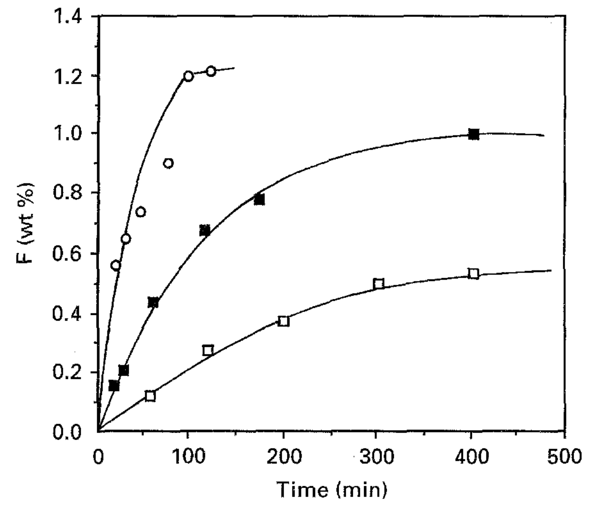

Figure 6 Time dependence of fluorine content. ○ 1229° C; ■ 1133° C; □ 1003° C.

$[SiO_{1.5}F]$.

$$d[SiO_{1.5}F]/dt = k_1[SiF_4]^n - k_2[SiO_{1.5}F]^m \quad (6)$$
$$k_1 = k_{(0)} \exp(E_a/RT)$$
$$k_2 = k_{2(0)} \exp(E_d/RT)$$

where $[SiO_{1.5}F]$ is the concentration of fluorine doped in solid after t minutes (wt %), $[SiF_4]$ is the SiF_4 gas ratio, k_1 is the rate coefficient of the doping reaction, k_2 is the rate coefficient of the dissociating reaction, E_a is an activation energy of the fluorine doping reaction (kcal mol^{-1}), E_d is an activation energy of the fluorine dissociating energy (kcal mol^{-1}), T is the temperature (K), n, m are the order's numbers and t is treatment time.

At the initial stage, the dissociation reaction can be negligible because $[SiO_{1.5}F]$ is very small. Then taking the latter term to be zero, we obtain a simplified expression as a substitute for Equation 6

$$d[SiO_{1.5}F]/dt = k_1[SiF_4]^n \quad (7)$$

At the equilibrium stage, the rate of the fluorine doping is the same as that of the dissociation, that is, Equation 6 equals zero; $d[SiO_{1.5}F]/dt = 0$. In this case, the actual doping is completed and Equation 6 is simply expressed as follows

$$[SiO_{1.5}F] = (k_1/k_2)^{(1/m)}[SiF_4]^{(n/m)} \quad (8)$$

Equations 7 and 8 show that all factors k_1, k_2, n and m for Equation 6 can be obtained by analysing the fluorine doping behaviour at the initial and equilibrium stages. That is, it is possible to examine the kinetic behaviour of the fluorine doping process, which can be expressed as Equation 6 obtained from analysing the fluorine doping behaviour at both initial and equilibrium stages.

4.2. Initial stage reaction

In order to investigate the initial stage reaction, the soot preforms were heatd for 22 min and their fluorine contents were estimated from the i.r. transmission spectra.

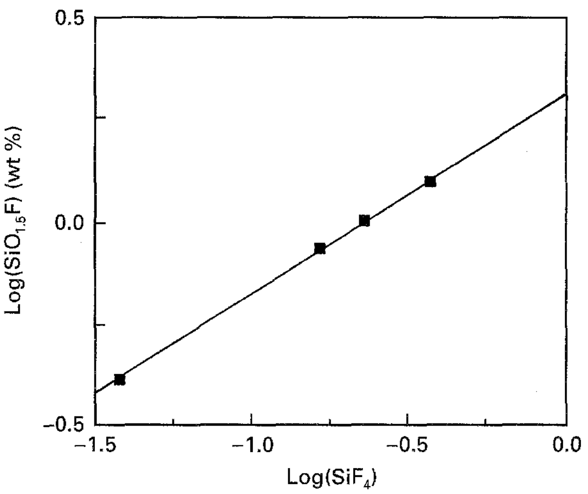

Figure 7 SiF_4 ratio dependence of fluorine content in glass.

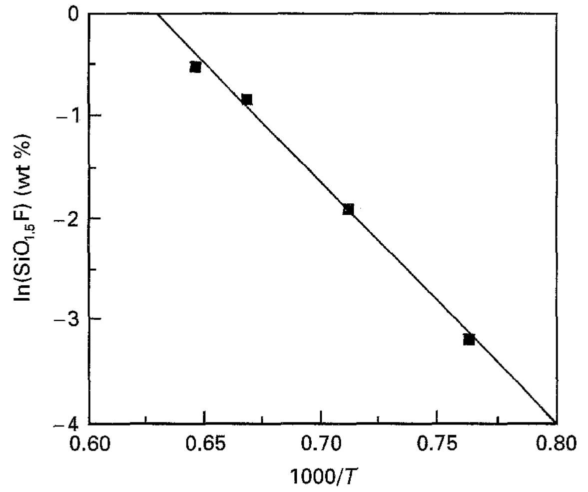

Figure 8 Arrhenius form of fluorine content in glass at initial stage.

Fig. 7 shows the SiF_4 gas ratio dependence on the fluorine content on a log–log scale. The soot preforms were heated at 1230 °C under various partial pressures of SiF_4.

The log of the fluorine content is found to be proportional to the SiF_4 gas ratio, indicating a power law $[SiO_{1.5}F] \propto [SiF_4]^b$ where $b = 0.50$. This correlation is simply expressed as follows

$$[SiO_{1.5}F] = 2.08 \times [SiF_4]^{0.50} \text{ (wt \%)} \quad (9)$$

Fig. 8 shows the Arrhenius form of the fluorine content. The soot was heated for 22 min under a SiF_4 partial pressure of 3.9 kPa. The activation energy was estimated to be 45.8 kcal mol^{-1} and the temperature dependence of the fluorine content is simply expressed as follows

$$[SiO_{1.5}F] = 2.09 \times 10^6 \times \exp(-45.8 \times 10^3/(RT)) \quad (10)$$

From Equations 9 and 10, the following equation was obtained

$$[SiO_{1.5}F] = 1.07 \times 10^7 \times [SiF_4]^{0.50} \times \exp(-45.8 \times 10^3/RT) \quad (11)$$

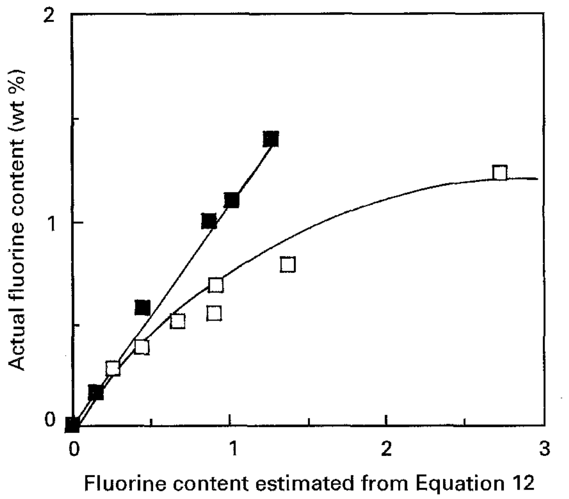

Figure 9 Relationship between experimental data and estimated values of fluorine content. ■ after 20 min; □ after 100 min.

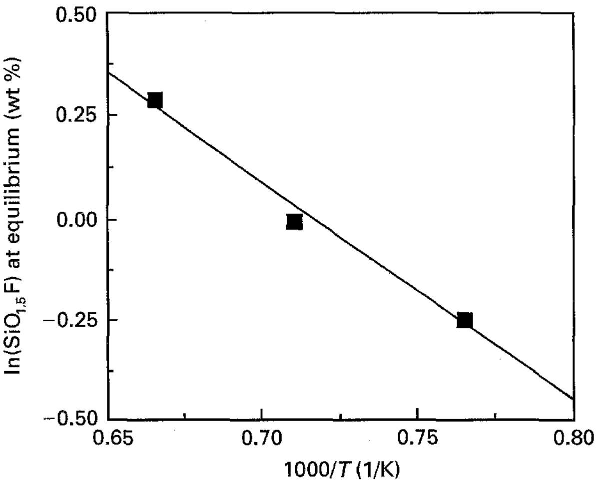

Figure 10 Arrhenius form of fluorine content in glass at equilibrium. $E_a = 10.8\ \text{kcal mol}^{-1}$.

The following differential equation was obtained by dividing the above equation by 22 min.

$$\mathrm{d}[\mathrm{SiO_{1.5}F}]/\mathrm{d}t = 4.84 \times 10^5 \times [\mathrm{SiF_4}]^{0.50} \times \exp(-45.8 \times 10^3/RT) \quad (12)$$

This equation shows that the fluorine doping rate is proportional to the 1/2 power of $[\mathrm{SiF_4}]$ and the activation energy is $45.8\ \text{kcal mol}^{-1}$.

Fig. 9 shows the relationship between the experimental data and the corresponding values estimated from Equation 12. The experimental data consisted of two groups; the data from 20 min doping and those from more than 100 min. The former corresponds to the initial stage and the latter to the other stages. At the initial stage, the experimental data are the same as the estimates. On the other hand, at the other stages, the experimental data were fairly smaller than estimated. This difference proves that the doping reaction followed by the dissociation reaction, as shown in Equation 6, took place at the other stages.

4.3. Equilibrium stage reaction

Fig. 10 shows the fluorine content data as a function of $1/T$. Those data were estimated by extrapolation to be approximately in equilibrium. The $\mathrm{SiF_4}$ partial pressure was 4.25 kPa. The fluorine content in equilibrium obeys the Arrhenius form and can be expressed as

$$[\mathrm{SiO_{1.5}F}] = 45.3 \times \exp(-10.8 \times 10^3/RT) \quad (13)$$

The activation energy is $10.8\ \text{kcal mol}^{-1}$. As already shown in Fig. 4, the fluorine content is proportional to the 1/4 power of the partial pressure. Equation 13 combined with the 1/4 power law of the $\mathrm{SiF_4}$ can be expressed as follows

$$[\mathrm{SiO_{1.5}F}] = 100 \times [\mathrm{SiF_4}]^{1/4} \times \exp(-10.8 \times 10^3/RT) \quad (14)$$

The power of 1/4 in Equation 14 corresponds to that of n/m in Equation 8 and the value of m is evaluated to be 2 as $n = 1/2$.

4.4. Formula of the fluorine doping behaviour

Using Equations 12 and 14, Equation 6 can be expressed as follows

$$\mathrm{d}[\mathrm{SiO_{1.5}F}]/\mathrm{d}t = k_1[\mathrm{SiF_4}]^{0.5} - k_2[\mathrm{SiO_{1.5}F}]^2 \quad (15)$$

The integrated form of Equation 15 is represented as

$$[\mathrm{SiO_{1.5}F}]t = (k_1/k_2)^{1/2} \times (a-1)/(a+1) \quad (16)$$

where $a = \exp[2(k_1k_2)^{1/2}t]$, $k_1 = 4.84 \times 10^5 \times [\mathrm{SiF_4}]^{1/2} \times \exp(-45.8 \times 10^3/RT)$ and $k_2 = 48.4 \times \exp(-24.6 \times 10^3/RT)$.

This kinetic equation describes all the stages of the fluorine doping behaviour.

5. Reaction mechanism

The kinetic investigation revealed that the fluorine doping process consists of the doping reaction and the dissociation reaction.

The doping reaction obeys the 1/2 power law of the $\mathrm{SiF_4}$ partial pressure, as shown in Equation 15. Then, based on the law of mass balance, the following chemical reaction can be derived

$$2\mathrm{SiO_2(s)} + \mathrm{SiF_4(g)} \rightarrow 2\mathrm{SiO_{1.5}F(s)} + \mathrm{SiOF_2(ad)} \quad (17)$$

where (g) is gaseous species, (s) is solids and (ad) is adsorbed species.

The species $\mathrm{SiOF_2}$ should be adsorbed on the $\mathrm{SiO_2}$ surface as shown in Fig. 11. $\mathrm{SiOF_2(g)}$ is known to be very unstable [13]. On the other hand, the XPS (X-ray photoelectron spectroscopy) study showed that the surface of a $\mathrm{SiO_2}$ wafer is covered with $\mathrm{SiOF_2}$

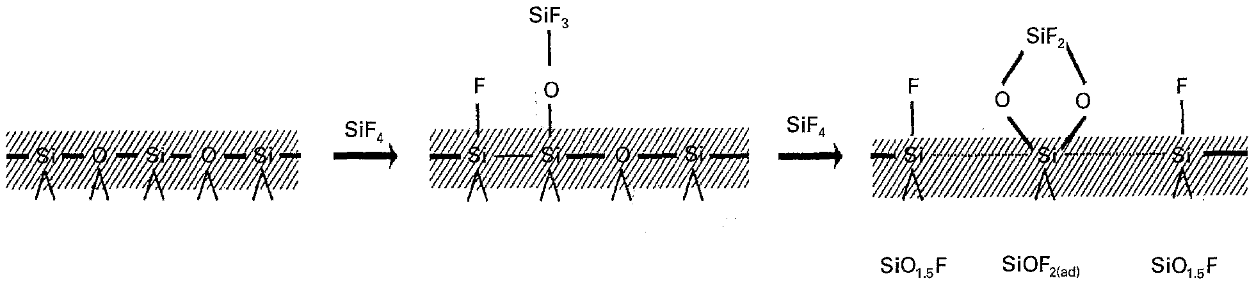

Figure 11 Model for fluorine doping mechanism.

after etching by NF_3 gas [14]. This fact supports the stability of $SiOF_2$(ad).

The dissociation reaction obeys the two power law of the concentration of $SiO_{1.5}F$. Then based on the law of mass balance, the following chemical reaction can be proposed

$$2SiO_{1.5}F(s) \rightarrow SiO_2(s) + SiOF_2(ad) \qquad (18)$$

$$2SiOF_2(ad) \rightarrow SiF_4(g) + SiO_2(s) \qquad (19)$$

The dissociation reaction consists of two steps and the rate of the first step should be slower than that of the second one. As a result, Equation 18 is the rate determinant one for the dissociation process.

At equilibrium, Equation 18 is in competition with Equation 13 and the overall reaction can be expressed as follows

$$3SiO_2(s) + SiF_4(g) = 4\,SiO_{1.5}F(s) \qquad (20)$$

The fluorine doping depends on the 1/4 power of the SiF_4 partial pressure and this dependency is the same as the empirical one as shown in Equation 2.

6. Conclusion

The fluorine doping reaction during the VAD sintering process was investigated. The kinetic investigation of this process has revealed the mechanism of fluorine doping.

This investigation clarified that the index depression is proportional to the 1/4 power of the fluorine gas partial pressure for any gas species such as SF_6, CF_4, C_2F_6 and SiF_4. The reduction of -0.75% of the relative refractive index is achieved by this process.

The kinetic investigation showed that the fluorine doping process consists of the doping and dissociation reactions; the former reaction obey the 1/2 power of the SiF_4 partial pressure and the latter the two power of fluorine content $[SiO_{1.5}F]$. The fluorine content is proportional to the 1/4 power of the SiF_4 partial pressure at an equilibrium where the doping reaction is in competition with the dissociation reaction. The following equation of the fluorine content can be expressed

$$[SiO_{1.5}F] = 100 \times [SiF_4]^{1/4} \times \exp(-10.8 \times 10^3/RT)(\text{wt}\,\%)$$

Acknowledgements

The authors wish to thank Dr M. Watanabe, N. Yoshioka and H. Yokota of Sumitomo Electric Industries Ltd., for their useful discussions.

References

1. S. SHIRAISHI, K. FUJIWARA and S. KUROSAKI, US Patent. 4082420 (1979).
2. K. ABE, in 2nd European Conference Optical Communication (IEE, Paris, 1976) p. 59.
3. A. KAWANA, T. MIYA, S. ARAKI and Y. FURUI, *Trans. IECEJ* **E65** (1982) 529.
4. K. RAU, A. MUHLICH and M. TREBER, in Technical Digest, Topical Meeting of Optical Fiber Transmission (Williamberg, 1977) p. TuC4-1.
5. H. YOKOTA, H. KANAMORI, G. TANAKA and K. YANO, in Proceeding of Eleventh European Conference Optical Communication (Venice, Italy, 1985) p. 77.
6 H. KANAMORI, H. YOKOTA, G. TANAKA, M. WATANABE, Y. ISHIGURO, I. YOSHIDA, T. KAKII, S. ITOH, Y. AASANO and S. TANAKA, *J. Lightwave Technol.* **LT-4(8)** (1986) 1133.
7. M. KYOTO, H. KANAMORI, N. YOSHIOKA, G. TANAKA and M. WATANABE, in Technical Digest MG5, Conference on Optical Fiber Communication (New Orleans, LA, 1984) p. 22.
8. M. KYOTO, Y. OHOGA, S. ISHIKAWA and Y. ISHIGURO, *J. Mater. Sci.* **28** (1993) 2738.
9. M. KYOTO, Y. CHIGUSA, M. OHOE, H. GO, M. WATANABE, T. MATUBARA, T. YAMAMOTO and H. KANAMORI, *J. Lightwave Technol.* **10** (1992) 289.
10. M. ONISHI, Y. KOYANO, M. SHIGEMATSU, H. KANAMORI and M. NISHIMURA, in press.
11. K. TSUKUMA, N. YAMADA, S. KONDO, K. HONDA and H. SEGAWA, *J. Non-Crystal. Solids* **127** (1991) 191.
12. M. KYÓTO, H. KANAMORI, G. TANAKA, Y. YOSHIOKA and H. GOTO, in Semiconductor and Material IEICE Japan (Tokyo, Japan, 1984) p. 1143 (In Japanese).
13. H. SCNOCKEL, *J. Molec. Struc.* **65** (1980) 115.
14. S. YOKOYAMA, Y. YAMAKAGE and M. HIROSE, *Appl. Phys. Lett.* **46** (1985) 1398.

Received 18 January 1994
and accepted 20 November 1995